Energy balance and heating mechanisms of the Martian Upper atmosphere with the NASA Ames MGCM.

L. Gkouvelis, A.S. Brecht, A. Kling, R.J. Wilson, C.E. Harman, M.A. Kahre, R.A. Urata & the MCMC team

NASA/Ames Research Center, Moffet Field, Mountain view, CA, USA

Overview

The present middle/upper Martian atmosphere, above ~80 km, connects the deep atmosphere to the Martian space environment. This region is important to understand for many reasons; evolution of atmospheres, comparisons to other planetary atmosphere, and mission development. The middle/upper atmosphere is known to be influenced by the lower atmosphere (water cycle, dust cycle, waves, etc. [2]) and the solar environment (solar magnetic activity, solar events). It contains the upper branch of the overturning meridional circulation and where the main heat source transitions from near-Infrared to ultraviolet radiation. Upward propagating tides have been seen to have an impact on upper atmospheric structure, such as nonmigrating tides which include diurnal and semidiurnal periodicities [1]. The location of these mechanisms strongly influences the atmospheric composition and dynamics that also connect to the numerous escape processes that drive the atmospheric volatile evolution [3]. These influences feed on a primitive property of an atmosphere; temperature. **This project focuses on individual radiative processes that drive the Martian's thermal structure above ~80 km as a function of latitude and season.**

This poster is a progress report on the model development needed for the project; specifically, the on-going work on vertically extending the NASA Ames Mars Global Climate Model (MGCM) utilizing the NOAA/GFDL FV3 dynamical core will be discussed (see table 1).

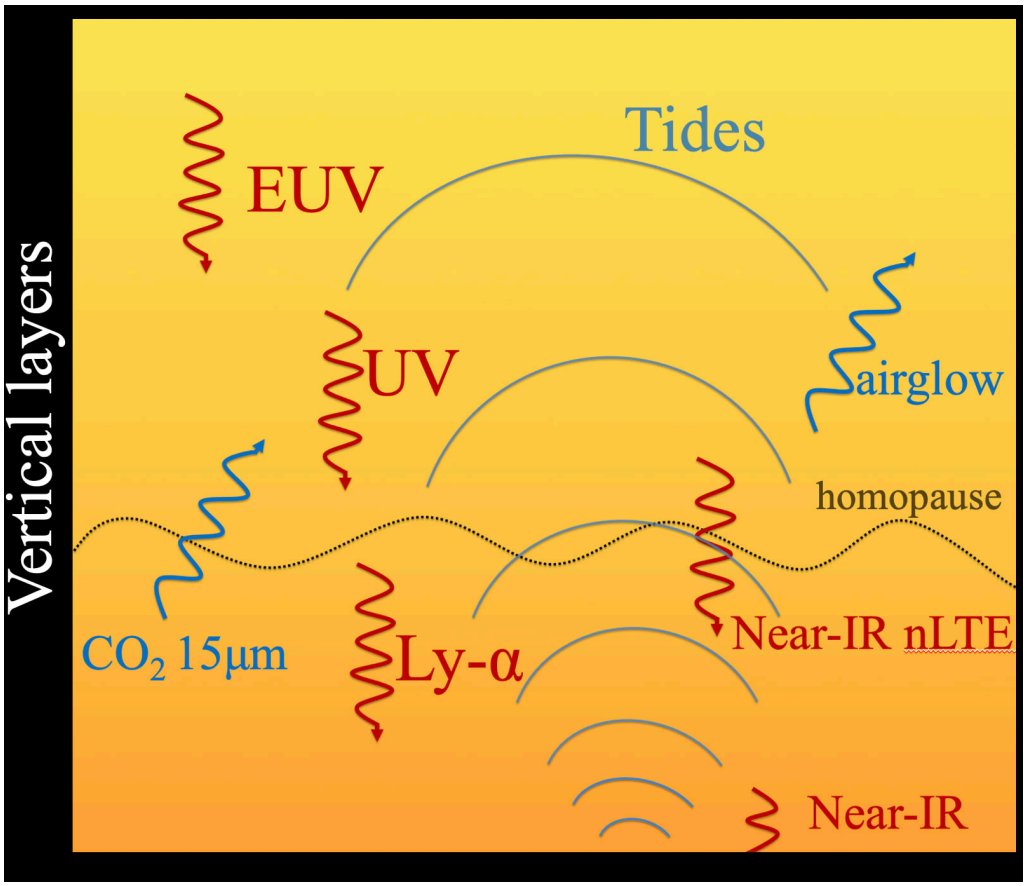

The MGCM nominally extends from the surface up to ~80 km but new physics packages will extend the MGCM's vertical domain up to ~250 km. We present the heating and cooling mechanisms that dominate this atmospheric region, discuss the parametrizations used and the state of the thermal structure. The main driving processes of the energy balance are the ultraviolet heating, thermal conduction and the 15 m cooling by CO_2. These processes will influence the temperature, photochemistry, and circulation of this region. Finally, we discuss the work in progress for the development of physics schemes and implementation in our model.

	Model Top	Thermal Terms	Other
Nominal	80 km	Near-IR (LTE/NLTE), CO2 15 micron (NLTE), dynamical	LMD lower atmosphere chemical package
New	150 km	Ultraviolet	
Next	250 km	Conduction, molecular viscosity	Upper atmosphere chemical package

Table 1: Description of the physical packages implemented and to be implemented in the near future.

The energy balance for middle and upper atmosphere can be described from:

$$\frac{\partial T}{\partial t} = Q_{UV} + Q_{near\ IR} + Q_{CO_2 15\mu m} + Q_{dynamics} + Q_{cond} \quad (1)$$

Were the left part of the equation is the temperature over time in Kelvin, Q_{UV} and Q_{IR} the total absorbed energy transformed into heating from the Ultraviolet and infrared parts of the spectrum. The IR is corrected for non-LTE accordingly. $Q_{CO2\text{-}15\,m}$ is the 15micron emission from excited CO_2. The $Q_{Dynamics}$ contains all the heating that is produced locally from the circulation. Both advection and adiabatic heating are summed up in this term. The last term of the equation (1) describes the heat diffusion equation were is the conductivity of the local mixing ratio and z is the vertical layer.

1. UV heating

Above ~80km the main incoming energy source is the absorption of solar Ultraviolet radiation from 0.1 to 200 nm. The amount of energy strongly depends on the solar magnetic eleven-year cycle. We calculate the total UV heating by solving equation (2):

$$\frac{\partial Q}{\partial t} = \epsilon \frac{1}{\rho C_p} \frac{\partial \Phi}{\partial z} \quad (2)$$

were Φ is the total photoabsorption rate for each spectral wavelength bin, z is the vertical layer and is the neutral heating efficiency. describes the portion of the total absorbed energy that will transform in atmospheric heating. Generally, the absorption of UV energetic photons will excite, dissociate and ionize the molecules of the atmosphere. Those processes will release energetic electrons as a byproduct which with their turn can result to the same interactions with the atmospheric constituents as well as to trigger chemical reactions that can

release energy. Detailed simulations have shown that only a fraction of the total energy will end up as heating in the order of 22% [4]. To properly account for solar UV irradiance at the top of the atmosphere we have adopted the FISM solar spectrum model [5] which is a detailed spectrum constructed with 1-nm resolution based on observations from The Extreme Ultraviolet Monitor (EUVM) spectrograph on board MAVEN and is collecting solar energy in three bands [7].

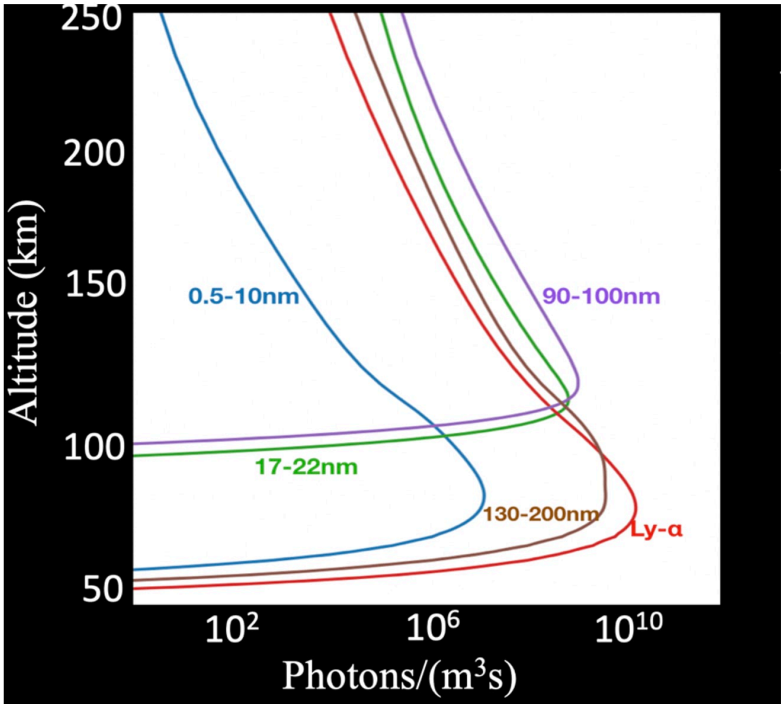

Figure1:Vertical penetration of the Photoabsorption from various ultraviolet spectral bands into the Martian atmosphere for SZA of 10° and medium solar activity.

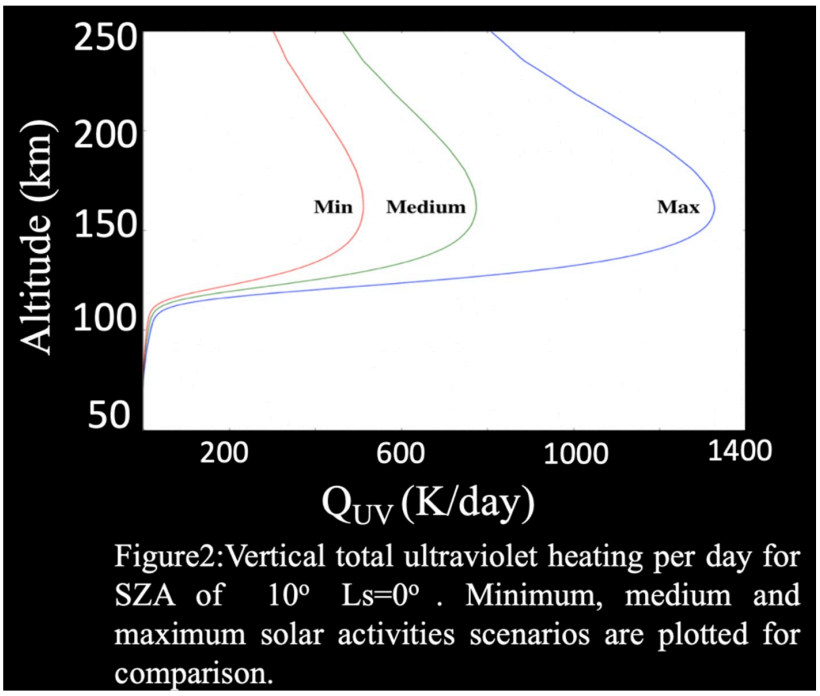

Figure2:Vertical total ultraviolet heating per day for SZA of 10° Ls=0° . Minimum, medium and maximum solar activities scenarios are plotted for comparison.

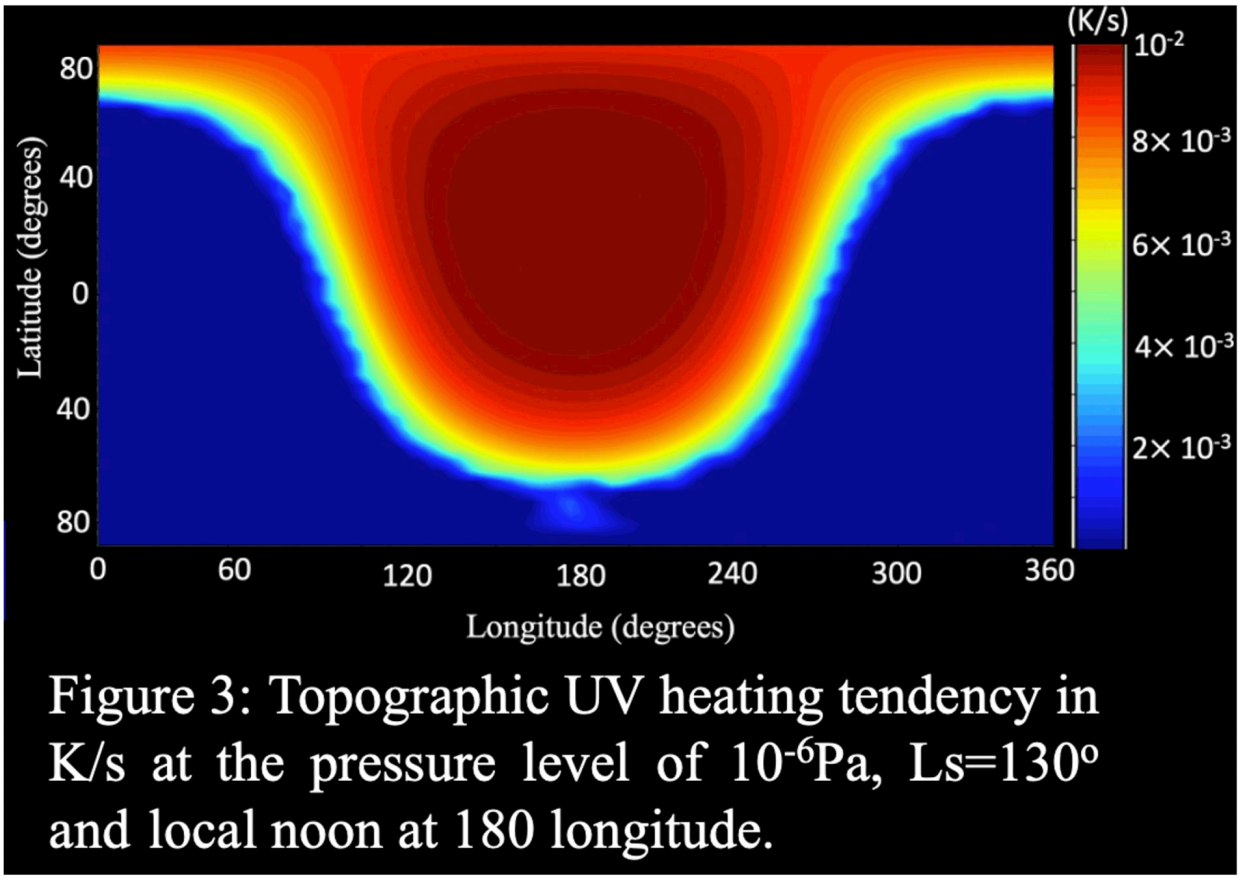

Figure 3: Topographic UV heating tendency in K/s at the pressure level of 10^{-6}Pa, Ls=130º and local noon at 180 longitude.

Temperature field

We are currently able to simulate up to the 10^{-6}Pa (~160km) and we show preliminary zonal mean temperature fields of three different epochs in figure 5, utilizing solar maximum conditions. The development and implementation of physical packages is ongoing process with our final objective to be able to cover up to ~250km. Parallel to model extension development comparison with modern observations of the middle and upper atmosphere are scheduled similar to [11], [12]. Figure 5 shows that the main dependece of the temperature field and the heating mechanisms is the distance from the sun and the inclination of the planet.

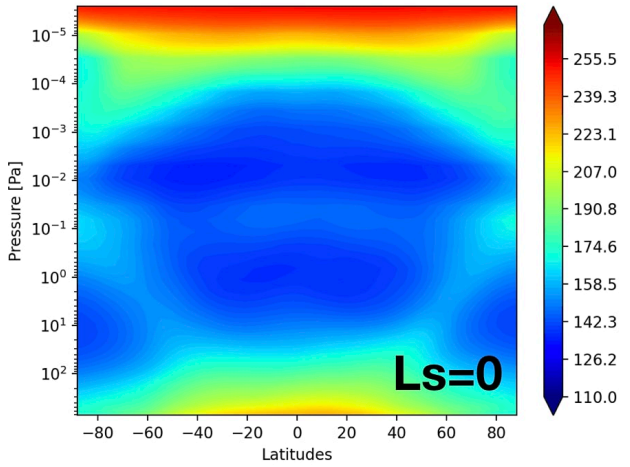
Ls=0
Pressure [Pa]
Latitudes
255.5
239.3
223.1
207.0
190.8
174.6
158.5
142.3
126.2
110.0

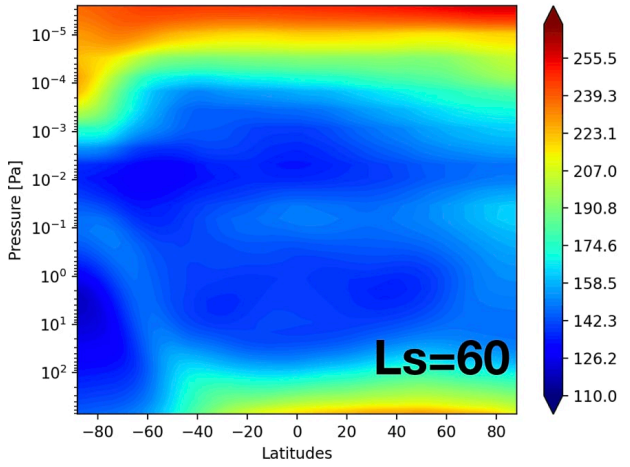
Ls=60
Pressure [Pa]
Latitudes
255.5
239.3
223.1
207.0
190.8
174.6
158.5
142.3
126.2
110.0

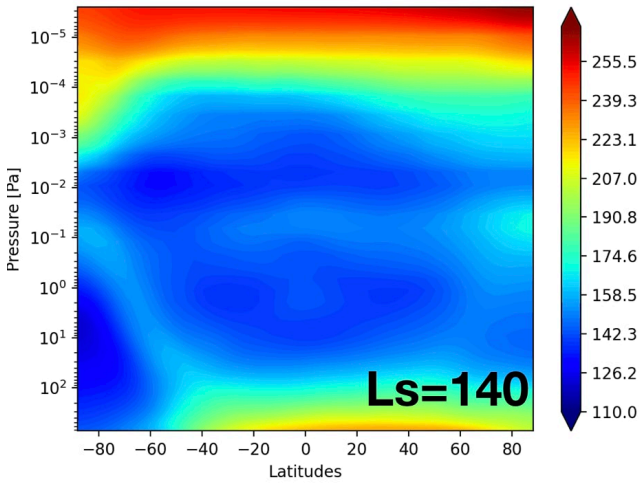
Ls=140
Pressure [Pa]
Latitudes
255.5
239.3
223.1
207.0
190.8
174.6
158.5
142.3
126.2
110.0

Figure 4: Temperature zonal mean fileds of three different solar longitudes followed by zonal mean heating tendencies

Heating terms

In the following figures we present basic zonal mean fields of the heating and cooling mechanisms for three Solar longitudes, same as figure 4. Scaling has been kept the same for all plots for comparison purposes.

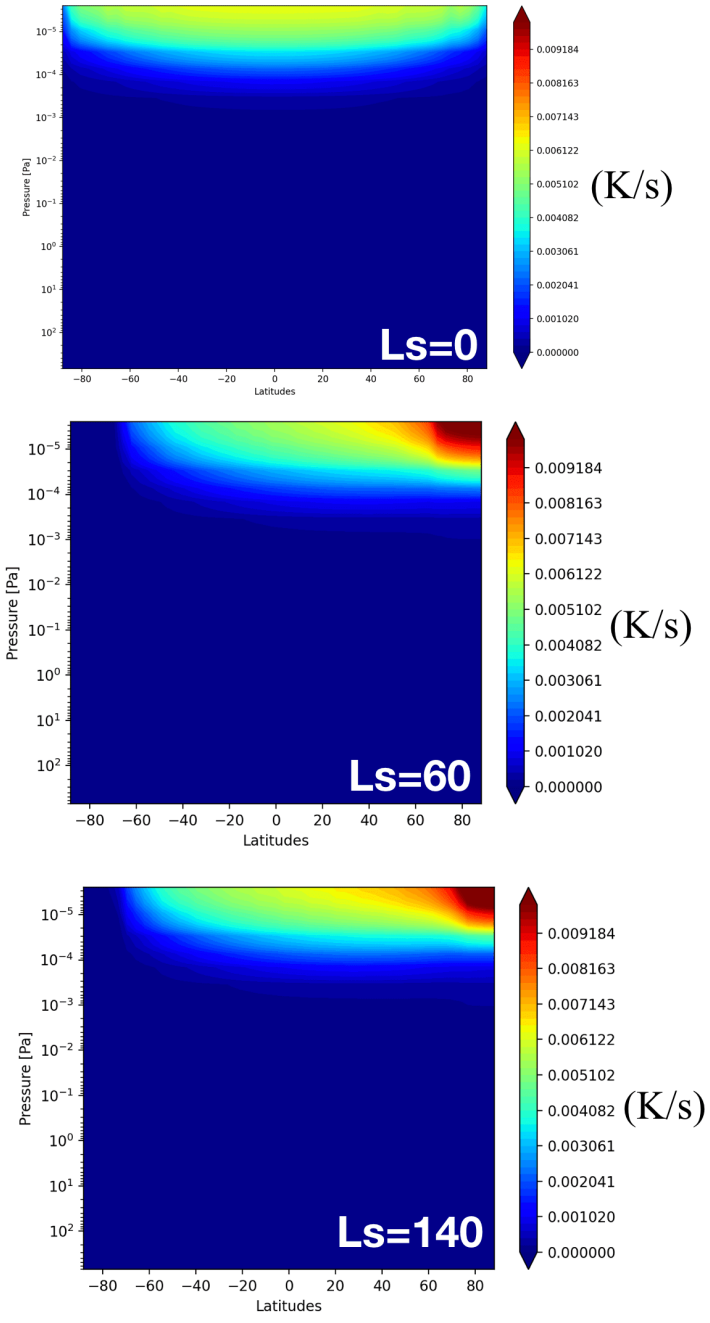

Figure 6: Equatorial zonal mean Ultraviolet heating in (K/s).

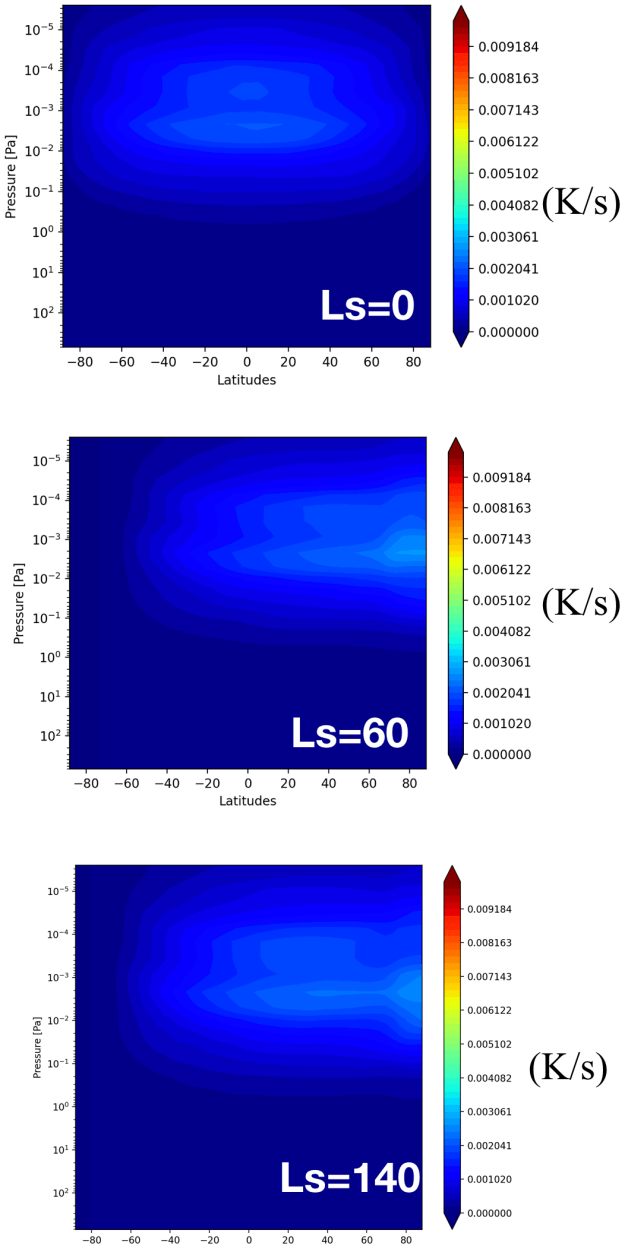

Figure y: Equatorial zonal mean Near IR heating in (K/s).

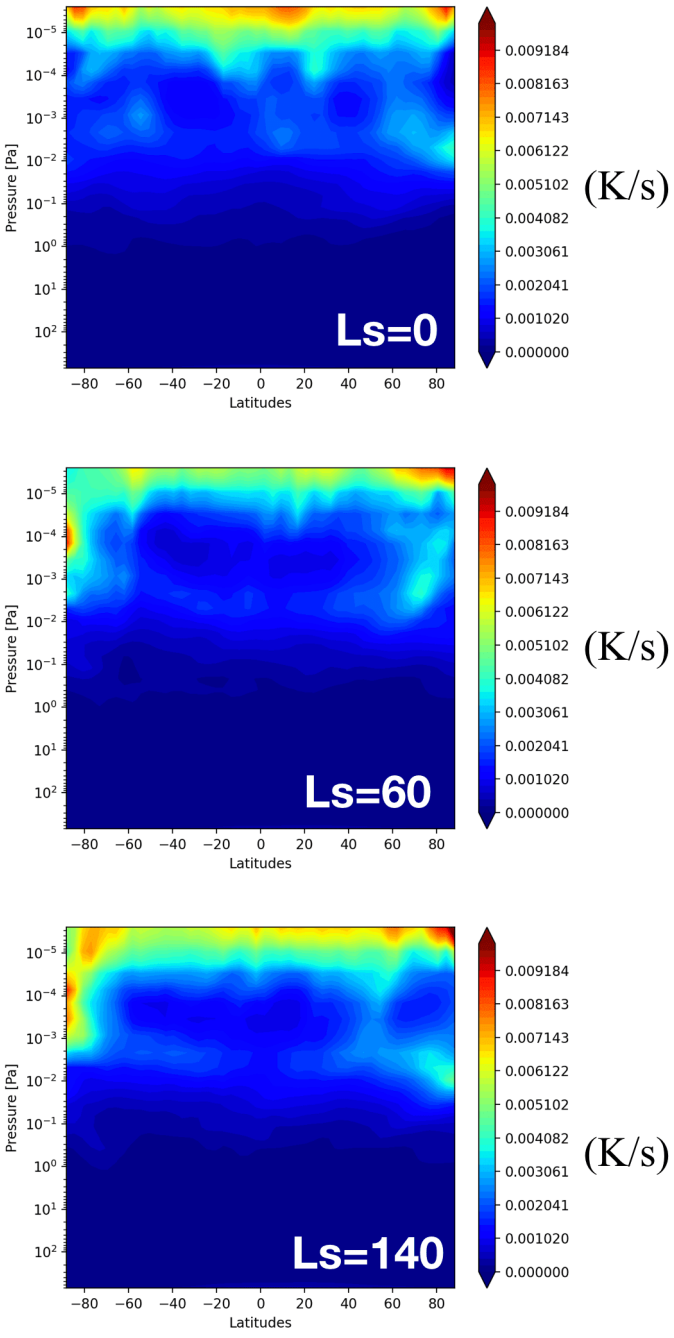

Figure 8: Equatorial zonal mean IR cooling in (K/s) after NonLTE corrections.

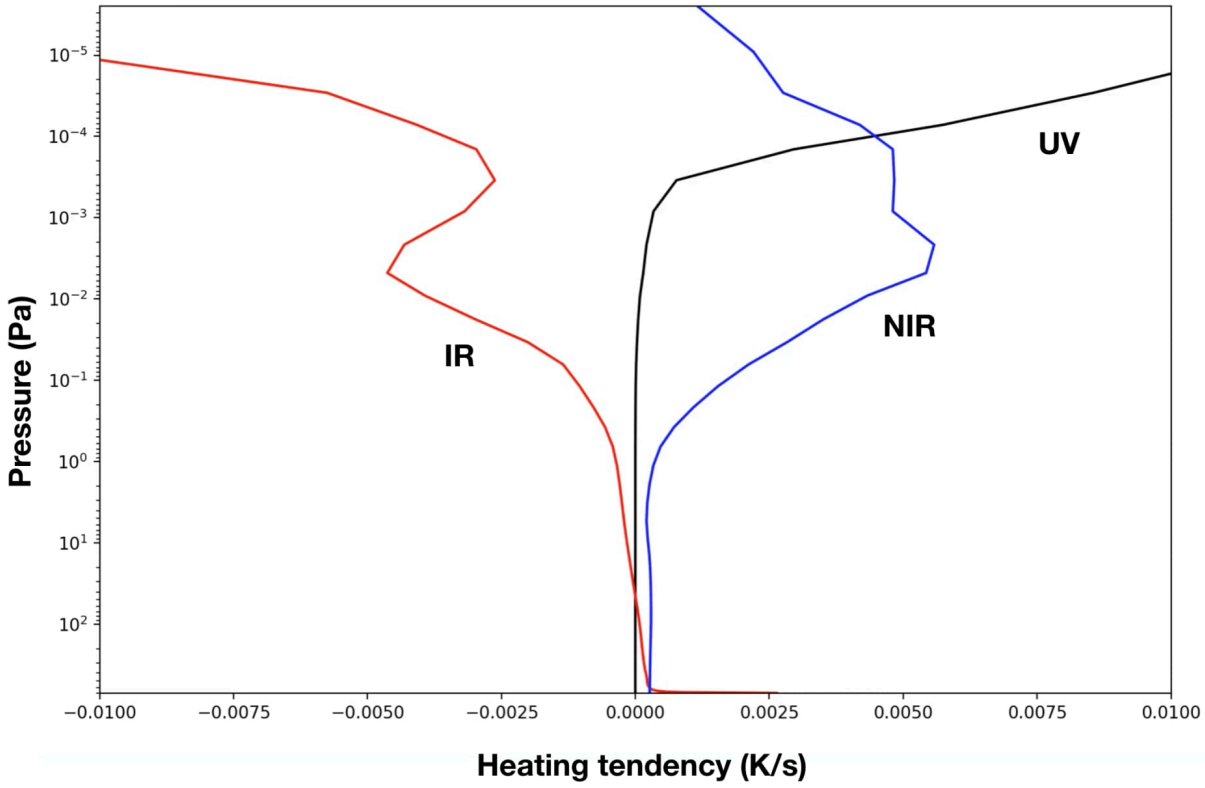

Figure 9: Typical daytime heating mechanisms of the radiation terms in the energy balance for the Martian Middle to upper atmosphere.

Thermal conduction, IR heating and CO2 15 m cooling

In the upper atmosphere of Mars thermal conduction is the main cooling mechanism. Heat is propagating to lower altitude layers and it is mainly transported through collisions into CO_2 molecules which are getting excited into higher levels and through relaxation emit long wave radiation back to space (See previous section on CO_2 15 m cooling). We discretize the thermal diffusion equation in order to calculate the heating tendency through conduction.

$$\frac{\partial T}{\partial t} = \frac{\partial}{\partial z} k \frac{\partial T}{\partial z} \quad (3)$$

Where the terms are described from equation (1), $k = AT^{0.69}$, following [8] and A a number density weighted average of the individual

thermal conductivities. The NonLTE correction to LTE is applied for altitudes higher then ~80km for near IR heating rates and NLTE CO_2 15 m cooling adopting the scheme that is presented at [9]. To properly account for cooling CO_2 15 m cooling conditions we need to realistic CO_2 abundances, atomic oxygen abundances and the collision excitation rate coefficient [10]. While thermospheric O abundance is poorly measured and recent observations present high seasonal variability and a mixing ratio of 3% with CO_2 at ~130km [6].

1. References

[1] Forbes, J. M., Zhang, X., Forget, F., Millour, E., & Kleinböhl, A. (2020). Solar tides in the middle and upper atmosphere of Mars. *Journal of Geophysical Research: Space Physics*, *125*

[2] Gkouvelis, L., Gérard, J. C., González-Galindo, F., Hubert, B., & Schneider, N. M. (2020). Isobar Altitude Variations in the Upper Mesosphere Observed With IUVS-MAVEN in Response to Martian Dust Storms. *Geophysical Research Letters*, *47*(12)

[3] Lillis, R.J., Brain, D.A., Bougher, S.W., Leblanc, F., Luhmann, J.G., Jakosky, B.M., Modolo, R., Fox, J., Deighan, J., Fang, X., Wang, Y.C., Lee, Y., Dong, C., Ma, Y., Cravens, T., Andersson, L., Curry, S.M., Schneider, N., Combi, M., Stewart, I., Clarke, J., Grebowsky, J., Mitchell, D.L., Yelle, R., Nagy, A.F., Baker, D., Lin, R.P., 2015. Characterizing Atmospheric Escape from Mars Today and Through Time, with MAVEN. Space Sci. Rev. 195, 357–422.

[4] Gu, H., Cui, J., Niu, D. D., Cao, Y. T., Wu, X. S., Li, J., ... & Wei, Y. (2020). Neutral heating efficiency in the dayside Martian upper atmosphere. *The Astronomical Journal*, *159*(2), 39..

[5] Thiemann, E. M., Chamberlin, P. C., Eparvier, F. G., Templeman, B., Woods, T. N., Bougher, S. W., & Jakosky, B. M. (2017). The MAVEN EUVM model of solar spectral irradiance variability at Mars: Algorithms and results. Journal of Geophysical Research: Space Physics, 122(3), 2748-2767.

[6] Ritter, B., Gérard, J.-C., Gkouvelis, L., Hubert, B., Jain, S. K., & Schneider, N. M. (2019). Characteristics of Mars UV dayglow emissions from atomic oxygen at 130.4 and 135.6 nm: MAVEN/IUVS limb observations and modeling. Journal of Geophysical Research: Space Physics, 124, 4809–4832

[7] Eparvier, F. G., Chamberlin, P. C., Woods, T. N., & Thiemann, E. M. B. (2015). The solar Extreme Ultraviolet Monitor for MAVEN. Space Science Reviews, 195(1–4), 293–301.

[8] González-Galindo, F., Forget, F., López-Valverde, M. A., Angelats i Coll, M., and Millour, E. (2009), A ground-to-exosphere Martian general circulation model: 1. Seasonal, diurnal, and solar cycle variation of thermospheric temperatures, *J. Geophys. Res.*, 114, E04001

[9] López-Valverde, M. A., Edwards, D. P., López-Puertas, M., & Roldán, C. (1998). Non-local thermodynamic equilibrium in general circulation models of the Martian atmosphere 1. Effects of the local thermodynamic equilibrium approximation on thermal cooling and solar heating. (E7), 16799-16811.*103*, *Journal of Geophysical Research: Planets*

[10] Bougher, S. W., D. A. Brain, J. L. Fox, F. González-Galindo, C. Simon-Wedlund, and P. G. Withers (2014a), Upper atmosphere and ionosphere, in *Mars II*, edited by B. Haberle et al., Cambridge Univ. Press, Cambridge, U. K.

[11] Gérard, J. C., Gkouvelis, L., Ritter, B., Hubert, B., Jain, S. K., & Schneider, N. M. (2019). MAVEN-IUVS observations of the CO2+ UV dou- blet and CO Cameron bands in the Martian thermosphere: Aeronomy, seasonal, and latitudinal distribution. *Journal of Geophysical Research: Space Physics*, *124*, 5816–5827. https://doi.org/10.1029/2019ja026596

[12] Gkouvelis, L., Gérard, J. C., Ritter, B., Hubert, B., Schneider, N. M., & Jain, S. K. (2020). Airglow remote sensing of the seasonal variation of the Martian upper atmosphere: MAVEN limb observations and model comparison. *Icarus*, *341*. 113666.https://doi.org/10.1016/j. icarus.2020.113666